Substituent Effects on Haptotropic Rearrangements of Bis(indenyl)zirconium Sandwich Complexes

Luis F. Veiros*

Centro de Química Estrutural, Complexo I, Instituto Superior Técnico, Avenida Rovisco Pais 1, 1049-001 Lisbon, Portugal

Received December 21, 2005

DFT/B3LYP calculations with a VDZP basis set were used to study the mechanism of interchange between the two inequivalent indenyl ligands (Ind′ = $C_6H_5R_2$) in η^5/η^9 sandwich complexes, [Zr(η^5-$C_6H_5R_2$)(η^9-$C_6H_5R'_2$)], as a function of the indenyl substituent (R, R′ = H, CH_3, SiH_3; R and R′ on the 1,3-indenyl carbons). The results indicate that haptotropic shifts and, consequently, the ligand interchange process are more favorable in complexes with silylated indenyls than in complexes with alkylated ligands. Both electronic and steric effects play an important role in the rearrangement process, determining the differences found for the two types of substituents. On one hand, alkylated indenyls show a preference for η^9-coordination over their silylated counterparts, resulting in stronger metal−(η^9-Ind′) bonds, more stable complexes, and ground-state stabilization of the η^5/η^9 species. On the other hand, interligand steric repulsion is considerably higher for complexes with alkylated ligands than for silylated analogues due to shorter C−C(R,R′) and C−H bond lengths, in comparison with the corresponding Si−C and Si−H distances. This effect is particularly important in the η^5/η^5 intermediates of the ligand interchange process, given the geometrical proximity of Ind′ substituents in those species. This results in less stable η^5/η^5 complexes in the case of alkylated indenyls, with a consequent rise in the energy profile of the rearrangement and lower reaction rates. For the THF adducts with mixed indenyl ligands, [Zr{η^6-($C_6H_5R_2$)}{η^5-($C_6H_5R'_2$)}(THF)] (THF = OC_4H_8), the stability difference between haptomers is considerably attenuated, compared to the one found in the parent sandwich complexes. In these species, a tuning of the Zr−O bond allows the partial balance of the metal electronic needs.

Introduction

Sandwich complexes occupy a prominent place in transition metal chemistry since the discovery of ferrocene, [$FeCp_2$] (Cp = $C_5H_5^-$, cyclopentadienyl).[1] Group 4 metal complexes are no exception to this rule, being of special interest given their reactivity in many important catalytic processes,[2] C−H and small molecule activation,[3−5] organic coupling,[2,6] and even dinitrogen trapping.[3,7−11]

Indenyl (Ind = $C_9H_7^-$) is a widely used π ligand, known to form sandwich complexes as illustrated by the synthesis of the bis(Ind) species of iron and cobalt.[12] These examples point to a parallel between Cp and Ind as ancillary ligands in organo-transition metal chemistry that is, now, completely established by the tremendous amount of fully characterized complexes where Ind coordinates the metal center by the five-membered ring, i.e., in a general η^5 mode.[13] However, regardless of the large number of well-documented examples where a η^5-Cp coordination is equivalent to a η^5-Ind one,[14] the differences between the reactivity of the corresponding complexes are, in many cases, striking. This a direct consequence of the long known coordination versatility of indenyl.[15] For example, the ability of adapting the number of M−C(Ind) bonds to the metal electronic needs, a characteristic of indenyl, is the basis of the enhanced reactivity of Ind complexes toward ligand substitution reactions, when compared to their Cp analogues. This is, perhaps, the more relevant example of the differences between the two ligands, from the historical point of view, being the origin of the expression "indenyl effect".[16]

Very recently, the isolation[17] and full structural characterization[18] of [Zr(Ind′)$_2$] complexes (Ind′ = 1,3-substituted indenyls, see Scheme 1), by Paul Chirik's group, provided some of the few known examples of sandwich complexes of group 4

* E-mail: veiros@ist.utl.pt. Phone: +351-218 419 283. Fax: +351-218 464 457.

(1) Crabtree, R. H. *The Organometallic Chemistry of the Transition Metals*, 3rd ed.; John Wiley and Sons: New York, 2001; p 129.
(2) Negishi, E.-I.; Takahashi, T. *Acc. Chem. Res.* **1994**, *27*, 124.
(3) Fryzuk, M. D. *Chem. Rec.* **2003**, *3*, 2.
(4) Fryzuk, M. D.; Johnson, S. A. *Coord. Chem. Rev.* **2000**, *200*, 379.
(5) Brintzinger, H. H.; Bercaw, J. E. *J. Am. Chem. Soc.* **1970**, *92*, 6182.
(6) Rosenthal, U.; Pellny, P.-M.; Kirchbauer, F. G.; Burkalov, V. V. *Acc. Chem. Res.* **2000**, *33*, 119.
(7) Berry, D. H.; Procopio, L. J.; Carroll, P. J. *Organometallics* **1988**, *7*, 570.
(8) Hanna, T. E.; Lobkovsky, E.; Chirik, P. J. *J. Am. Chem. Soc.* **2004**, *126*, 14688.
(9) Horácek, M.; Stepnicka, P.; Kubista, J.; Fejfarová, K.; Gyepes, R.; Mach, K. *Organometallics* **2003**, *22*, 861.
(10) Pool, J. A.; Lobkovsky, E.; Chirik, P. J. *J. Am. Chem. Soc.* **2003**, *125*, 2241.
(11) Gell, K. I.; Schwartz, J. *J. Am. Chem. Soc.* **1981**, *103*, 2687.
(12) Pauson, P. L.; Wilkinson, G. *J. Am. Chem. Soc.* **1954**, *76*, 2024.
(13) Allen, F. H. *Acta Crystallogr.* **2002**, *B58*, 380.
(14) A closer inspection of the Ind coordination reveals that, in most cases, it is better described as $\eta^3+\eta^2$ with three short and two long M−C bonds. See, for example: Calhorda, M. J.; Veiros L. F. *Coord. Chem. Rev.* **1999**, *185−186*, 37.
(15) O'Connor, J. M.; Casey, C. P. *Chem. Rev.* **1987**, *87*, 307.
(16) For a recent reinterpretation of the indenyl effect and a comprehensive reference list on the subject, see: Calhorda, M. J.; Romão, C. C.; Veiros, L. F. *Chem. Eur. J.* **2002**, *8*, 868.
(17) Bradley, C. A.; Lobkovsky, E.; Chirik, P. J. *J. Am. Chem. Soc.* **2003**, *125*, 8110.
(18) Bradley, C. A.; Keresztes, I.; Lobkovsky, E.; Young, V. G.; Chirik, P. J. *J. Am. Chem. Soc.* **2004**, *126*, 16937.

10.1021/om051085l CCC: $33.50
Publication on Web 03/29/2006

Scheme 1

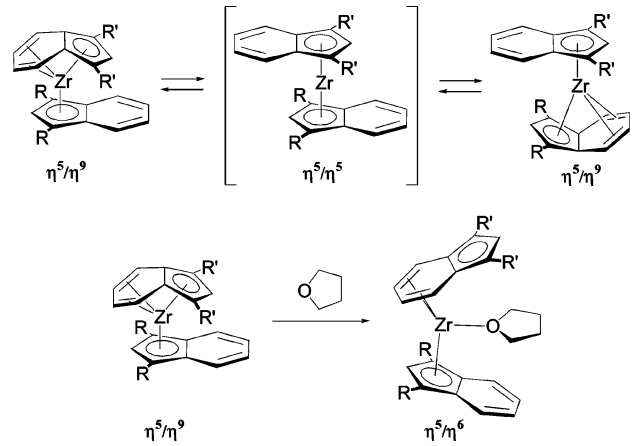

metals.[19−21] These bis(Ind′)zirconium complexes present some interesting characteristics concerning both structure and reactivity. The two Ind′ ligands are inequivalent; one is coordinated in the common η^5 mode, but the other is bonded through its entire π system, in an unprecedented η^9 mode. In addition, a fluxional process occurring in solution was experimentally observed,[17] corresponding to the interchange between the two differently coordinated ligands and implying, thus, the existence of haptotropic shifts between η^5-Ind′ and η^9-Ind′. The reactivity of the Zr sandwich complexes toward the addition of σ donors, such as THF (OC_4H_8), is also surprising, yielding adducts [Zr(η^5-Ind′)(η^6-Ind′)(THF)],[17] with one Ind′ coordinated by the benzene ring, following an unusual η^9 to η^6 shift (Scheme 1).

The kinetics of the ligand interchange process was experimentally investigated, as a function of the Ind′ substituents, R and R′ (Scheme 1, top).[18] The results indicate an increased tendency to haptotropic shifts and, thus, ligand interchange, for electron-deficient molecules, but no definitive pattern could be established. Recently, an excellent study involving both the kinetics and the thermodynamics for the addition of σ donors to [Zr(η^5-Ind′)(η^9-Ind′)] sandwich complexes (Scheme 1, bottom) clearly demonstrated that, on one hand, for molecules with the same steric environment silylated Ind′ ligands induce more facile reactions than their alkylated analogues, while, on the other, for complexes with comparable electronic characteristics, an increase in the steric bulk of the Ind′ substituents disfavors the reaction.[22]

In a recent report, the structure and reactivity of [Zr(η^5-Ind)-(η^9-Ind)] sandwich complexes were thoroughly studied, using DFT calculations[23] and models with unsubstituted indenyl ligands.[24] Here, that work is extended to the influence of Ind′ substituents on the mechanism of the haptotropic shifts involved in the ligand interchange process. This way, the theory level employed is tested with respect to the simplicity of the models used, while the reasons behind the reactivity differences experimentally observed are better understood and systematized. The substituents studied (R, R′ = CH_3 and SiH_3) represent a compromise between computational limitations and fulfilment of the goals stated above. The results obtained allow not only conclusions on the influence of the electronic characteristics of the substituents on the reaction mechanisms, but also considerations on the role of steric effects in the same mechanisms.

Scheme 2

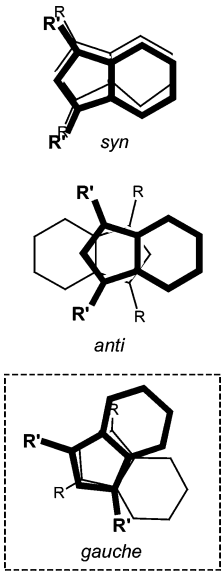

Results and Discussion

Ring Interconversion in [Zr(η^5-Ind′)(η^9-Ind′)] Sandwich Complexes. There are three limiting conformations for Zr bis-(Ind′) complexes, depending on the relative position of the ligands (Scheme 2): a *syn* conformation, with perfectly eclipsed indenyl ligands, an *anti* conformation where the benzene rings of the indenyls are opposite each other, and an intermediate, *gauche*, conformation. The interconversion between the different conformers can be achieved through rotation of the indenyl ligands. Given the small activation energies involved, Ind′ rotation occurs smoothly in solution, even after freezing the ligand interconversion process.[18,24] Small stability differences are, thus, to be expected between the conformers. This is corroborated by the determination of the X-ray structures of [Zr(η^5-Ind′)(η^9-Ind′)] complexes in the *anti* (R = R′ = $SiMe_2{}^t$-Bu) and in the *gauche* conformations (R = R′ = ^{i}Pr).[18] In addition, the mechanism of ligand interchange was studied in detail for each of the three conformers of the complex with unsubstituted indenyl, revealing no significant differences.[24] Therefore, the studies of the influence of the Ind′ substituents on the ligand interchange process, here reported, were performed considering only the *gauche* conformer of the different species. This is the conformation observed in the experimental structure of the [Zr(η^5-Ind′)(η^9-Ind′)] complex with the simplest indenyl substituent, isopropyl, and, consequently, the one that is closer to the models adopted (with CH_3 and SiH_3 substituents).

The more favorable mechanism for the interchange between η^5-Ind′ and η^9-Ind′ in Zr bis(Ind′) sandwich complexes involves η^5/η^5 species as intermediates.[24] Figure 1 presents a general energy profile for that mechanism. As the reaction proceeds, the indenyl ligand originally coordinated in a η^9 mode shifts to a η^5 coordination, while the other ligand follows the reverse process, i.e., a η^5 to η^9 shift. The mechanism for the interconversion is conceptually simple. Starting from complex **A**, for example, a shift of the top Ind′ ligand from the η^9 to the η^5 coordination mode results in a η^5/η^5 species (**B**) with two

(19) Hitchcock, P. B.; Kerton, F.; Lawless, G. A. *J. Am. Chem. Soc.* **1998**, *120*, 10264.
(20) Lukesová, L.; Horácek, M.; Stepnicka, P.; Fejfarová, K.; Gyepes, R.; Cisorová, I.; Kubista, J.; Mach, K. *J. Organomet. Chem.* **2002**, *663*, 134.
(21) Horácek, M.; Kupfer, V.; Thewalt, U.; Stepnicka, P.; Polásek, M.; Mach, K. *Organometallics* **1999**, *18*, 3572.
(22) Bradley, C. A.; Lobkovsky, E.; Keresztes, I.; Chirik, P. J. *J. Am. Chem. Soc.* **2005**, *127*, 10291.
(23) Parr, R. G.; Yang, W. *Density Functional Theory of Atoms and Molecules*; Oxford University Press: New York, 1989.
(24) Veiros, L. F. *Chem. Eur. J.* **2005**, *11*, 2505.

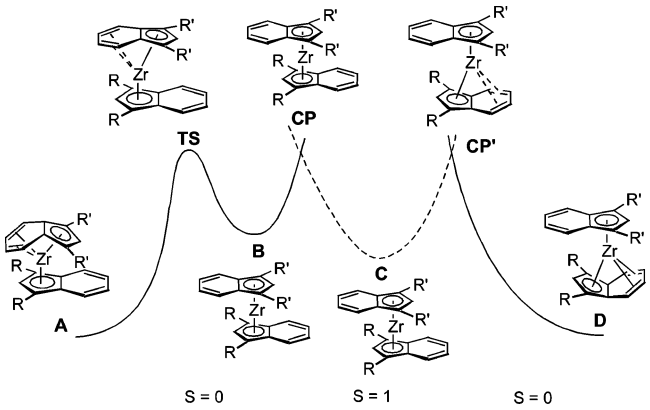

Figure 1. General energy profile for the interconversion mechanism of the indenyl ligands in [Zr(η^5-Ind′)(η^9-Ind′)]. The plain curves correspond to the spin singlet potential energy surface, PES ($S = 0$), and the dashed curve to the spin triplet ($S = 1$) PES.

symmetrically coordinated indenyl ligands. From **B**, a similar shift involving the other indenyl ligand produces the η^5/η^9 complex with interchanged ligands. The haptotropic shift that connects **A** and **B** goes through a transition state (**TS**) where the indenyl coordination is intermediate between η^9 and η^5, and the entire process occurs in the spin singlet potential energy surface (PES); that is, all the species involved are spin singlets ($S = 0$). However, it is well known[25] that the more stable spin state for a d^2 metallocene is a triplet ($S = 1$), and, consequently, the participation of a spin triplet η^5/η^5 complex (**C**), as an intermediate in the mechanism, had to be considered. A direct transformation of a η^5/η^9 complex (**D**, for example) in **C** corresponds to a "spin-forbidden" or "nonadiabatic" reaction since it involves a change in the spin state, starting with a singlet reactant and ending up in a triplet product. The energy profile of such a reaction goes through a minimum energy crossing point (MECP), which corresponds to the lowest energy point at which the energy and the geometry of the molecule is the same in the two surfaces, in this case the spin singlet and the spin triplet surfaces. Once the MECP is reached, the system has a given probability of changing its spin state and, thus, hopping from one surface to the other, completing the reaction.[26] In the reaction profile of Figure 1 the MECP connecting a η^5/η^9 complex (**D**) with the η^5/η^5 triplet species (**C**) is **CP′**. The haptotropic shift that transforms **D** into **C** is entirely equivalent, from the geometrical point of view, to the one that connects **A** and **B**. Both correspond to the shift of one indenyl ligand from the η^9 to the η^5 coordination mode, and both go through a species in which the shifting ligand presents a coordination mode intermediate between η^5 and η^9 (**TS** in the one case and **CP′** in the other). These two processes represent competitive pathways to the ligand interchange mechanism, and the preferred one will depend on the relative energy of **TS** and **CP′**. Finally, **CP**, the MECP for the interconversion between the two η^5/η^5 isomers, the spin singlet complex (**B**), and the spin triplet one (**C**), connects the two pathways described above and completes the energy profile represented in Figure 1.

The values for the relative energies of the relevant points in the reaction profile, for all the complexes studied, are presented in Table 1. The molecules studied can be divided in two classes. Complexes **1** and **2** have two identical Ind′ ligands, that is, R = R′, and provide a clear illustration of the differences between an alkylated (**1**) and a silylated (**2**) molecule. The last type of species considered has two different indenyl ligands (R ≠ R′), one unsubstituted, and the other alkylated (**3**/**3′**) or silylated (**4**/**4′**). Each of these last species will have two different profiles, one for the shift of each indenyl ligand, although with common points: the η^5/η^5 species, **B**, **CP**, and **C**. The consideration of complexes with two different ligands allows a direct comparison, among isomers, of the relative stability of each relevant point along the energy profile with substituted and unsubstituted ligands, for each type of substituent. The labeling scheme adopted in Table 1 for R and R′ corresponds to the one in Figure 1. The energy values of Figure 1 are relative to the most stable species for *each* energy profile (systems **1** to **4′**); in all cases this corresponds to the η^5/η^9 complex (**A** or **D**).

Table 1. Relative Energies (kcal mol^{-1}) for the Relevant Points of the Reaction Profile of Ind′ Interchange in [Zr(η^5-Ind′)(η^9-Ind′)] Sandwich Complexes

complex	R	R′	A	TS	B	CP	C	CP′	D
1	CH_3	CH_3	0	**12.2**	9.5	14.6	6.6	13.8	0
2	SiH_3	SiH_3	0	**10.4**	4.5	4.8	2.5	12.1	0
3	H	CH_3	0	**12.6**	9.7	12.8	6.8	14.9	1.4
3′	CH_3	H	1.4	**13.2**	9.7	12.8	6.8	14.1	0
4	H	SiH_3	0.7	**11.5**	6.6	7.7	4.2	13.5	0
4′	SiH_3	H	0	**11.6**	6.6	7.7	4.2	13.0	0.7

Two major conclusions can be drawn from the values in Table 1. The first is that, since **TS** is systematically more stable than **CP′**, the preferred pathway for the haptotropic shift is, in all cases, the one that follows the spin *singlet* PES. The rate-limiting step in this mechanism is the η^9 to η^5 shift, **A** → **TS** → **B**, and, consequently, **B** is the relevant intermediate in the process. The second conclusion is that the ligand interchange reaction has lower activation energies and, thus, is more facile for complexes with silylated indenyl ligands ($E_a = 10.4-11.6$ kcal mol^{-1}) than for molecules with alkylated ligands ($E_a = 12.2-13.2$ kcal mol^{-1}), in excellent agreement with the experimental findings.[18,22]

The differences in reactivity reflected in the values of Table 1 can be explained by two reasons. One is ground-state stability of the η^5/η^9 complexes. In fact, the comparison of the relative stability of the two isomers of **A** with only one methylated Ind′ (species **3** and **3′**) reveals, even for such a simple system, that the isomer with a η^9 coordination of the methylated indenyl is 1.4 kcal mol^{-1} more stable than the equivalent species with this ligand η^5 coordinated. The reverse happens for the complexes with only one silylated ligand (species **4** and **4′**), although the stability difference is lower (0.7 kcal mol^{-1}). This indicates that alkylated indenyl ligands, when coordinated in a η^9 mode, give rise to more stable complexes than their silylated counterparts in the same situation.

The second factor behind the reactivity differences expressed by the energy values in Table 1 is the relative stability of the η^5/η^9 complexes (**A**) versus the η^5/η^5 intermediates. Of these, the spin triplet species, **C**, are systematically more stable than their singlet isomers, **B**, as expected, and the trend in the relative stability of **B** and **C** is maintained for all the systems studied. However, the following discussion will be centered on **B** since this is the intermediate relevant for the haptotropic shift, being the one involved in the rate-limiting step of the mechanism (see above): **A** → **TS** → **B**. The destabilization experienced by the system in the process of going from the η^5/η^9 molecules (**A**) to the η^5/η^5 species (**B**) is considerably less pronounced for silylated molecules than for their alkylated equivalents. This is shown by the relative energy of intermediate **B** for the silylated complexes (4.5 and 6.6 kcal mol^{-1}), when compared with the

(25) Green, J. C. *Chem. Soc. Rev.* **1998**, *27*, 263.

(26) For excellent reviews on MECP and their location for transition metal complexes, see: (a) Harvey, J. N.; Poli, R.; Smith, K. M. *Coord. Chem. Rev.* **2003**, *238−239* , 347. (b) Poli, R.; Harvey, J. N. *Chem. Soc. Rev.* **2003**, *32*, 1.

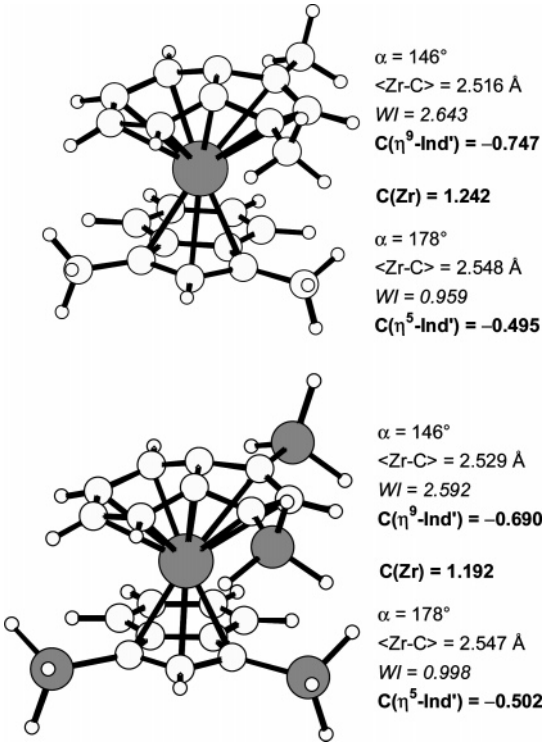

Figure 2. Optimized geometries (B3LYP) for [Zr(η^9-C_9H_5-1,3-CH_3)(η^5-C_9H_5-1,3-CH_3)] (top) and [Zr(η^9-C_9H_5-1,3-SiH_3)(η^5-C_9H_5-1,3-SiH_3)] (bottom). The more relevant geometrical and electronic parameters are presented: the NPA charge for the metal and each ligand (C, in bold), the folding angle of the ligand (α, in deg), the mean distance for all the Zr−C bonds (⟨Zr−C⟩, in Å), and the corresponding sum of Wiberg indices (WI, in italics). The Zr and Si atoms are shaded.

Scheme 3

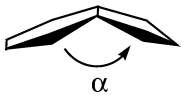

methylated analogues (9.5 and 9.7 kcal mol^{-1}). The combination of less stable η^5/η^9 complexes and more stable η^5/η^5 intermediates results in lower energy profiles for the haptotropic rearrangement of silylated molecules and, thus, more facile ligand interconversion processes. The energy of each transition state, **TS**, and, consequently, the activation energy of the reaction, reflects the energy of the two minima connected, **A** and **B**, verifying, by and large, Hammond's postulate (see below).

A deeper analysis of the reasons distinguishing the reactivity of silylated and alkylated complexes, discussed above, is better performed on the species with two substituted ligands, **1** and **2**, where the differences are more pronounced. Figure 2 shows the optimized structures of the η^5/η^9 species for both complexes, with the more relevant geometrical and electronic parameters. The coordination geometry of the two indenyl ligands is equivalent for the two complexes of Figure 2. In both there is one ligand coordinated in a η^5 mode, while the other establishes nine Zr−C bonds, in a η^9 geometry. The similarity between the two complexes is demonstrated by the folding angle (α) of the ligands, that is, the angle between the planes of the C_5 and the benzene rings of indenyl (Scheme 3). The η^5-Ind′ remains essentially planar (α = 178°), while the ligand η^9 coordinated is severely bent (α = 146°), but both molecules present the same values. Despite the general resemblance, from the geometrical point of view, some differences can be found between the Zr−Ind′ bond strength in the two complexes and are implicit in the parameters shown in Figure 2.

The bonding of a π ligand coordinated to a metal center in a η^5 mode is well known, being basically composed by three two-electron donations from the ligand to the metal.[25] In the case of a η^9-Ind′ ligand, besides the ligand to metal donations, there is an important contribution to the bonding arising from back-donation from the metal to the benzene ring of Ind′, resulting in the HOMO (highest occupied molecular orbital) for [Zr(η^5-Ind′)(η^9-Ind′)] sandwich complexes.[24] There is a synergetic effect in the overall bonding of these species, since stronger donors coordinated in a η^5 mode enhance the back-donation from the metal to the η^9 ligand, resulting in more stable molecules. For the complexes represented in Figure 2, the differences in the bonding of the two types of ligands can be related to the donor capabilities of each Ind′. Those are better seen for the η^5 coordination, where the bonding is essentially based on ligand to metal donations. Figure 2 shows the charge distribution between the metal and each ligand of the two complexes, obtained by means of a natural population analysis (NPA).[27] The alkylated Ind′ is a better donor than the silylated ligand since the η^5-Ind′ is less negative in **1** (Figure 2, top). However, the Zr−(η^5-Ind′) coordination is slightly stronger in the case of the silylated complex, as shown by the sum of the Wiberg indices (WI)[28] corresponding to the five Zr−C bonds. Although it may seem puzzling, at first, the reason a stronger bond is achieved with a weaker donor is due to shorter Zr−C bond lengths. In fact, silylated Ind′ ligands get closer to the metal than alkylated ligands and, thus, produce stronger Zr−(η^5-Ind′) bonds (see below the discussion on the bonding of the η^5/η^5 complexes, **B**). This is only perceptible in the Zr−C mean distances in Figure 2, where it is masked by a more slipped coordination mode of the silylated η^5-Ind′ ligand. The slippage parameters (Δ)[29] are 0.084 and 0.105 Å, for the alkylated and the silylated η^5-Ind′, respectively. In fact, the Zr−C distances for the three allylic carbons, the ones that bind more strongly to the metal,[30] are significantly shorter in the case of the silylated η^5-Ind′ (2.483, 2.494, and 2.539 Å) than in the case of the methylated ligand (2.496, 2.513, and 2.535 Å).

From the point of view of the haptotropic shift associated with the ligand interchange reaction, the more relevant aspect of the bonding in the molecules of Figure 2 is the coordination of the η^9 ligand, since this is the one that will undergo slippage process. There, a clear difference is found for the two species. The η^9-Ind′ coordination is stronger in the case of the alkylated molecule, as shown by shorter Zr−C distances and higher Wiberg indices. A more negative ligand indicates a more efficient back-donation from the metal to the η^9-Ind′, for the methylated complex. In fact, the enhanced back-donation in the

(27) (a) Carpenter, J. E.; Weinhold, F. *J. Mol. Struct. (THEOCHEM)* **1988,** *169*, 41. (b) Carpenter, J. E. Ph.D. Thesis, University of Wisconsin (Madison WI), 1987. (c) Foster, J. P.; Weinhold, F. *J. Am. Chem. Soc.* **1980**, *102*, 7211. (d) Reed, A. E.; Weinhold, F. *J. Chem. Phys.* **1983**, *78*, 4066. (e) Reed, A. E.; Weinhold, F. *J. Chem. Phys.* **1983**, *78*, 1736. (f) Reed, A. E.; Weinstock, R. B.; Weinhold, F. *J. Chem. Phys.* **1985**, *83*, 735. (g) Reed, A. E.; Curtiss, L. A.; Weinhold, F. *Chem. Rev.* **1988**, *88*, 899. (h) Weinhold, F.; Carpenter, J. E. *The Structure of Small Molecules and Ions*; Plenum: New York, 1988; p 227.

(28) (a) Wiberg, K. B. *Tetrahedron* **1968**, *24*, 1083. (b) Wiberg indices are electronic parameters related with the electron density between atoms. They can be obtained from a natural population analysis and provide an indication of the bond strength.

(29) (a) Faller, J. W.; Crabtree, R. H.; Habib, A. *Organometallics* **1985**, *4*, 929. (b) The slippage parameter (Δ) measures the slippage degree of a Ind ligand, being defined as the difference between (i) the Zr−C mean distance for the two hinge carbons and (ii) the mean distance between the metal and the three allylic carbons.

(30) Veiros, L. F. *Organometallics* **2000**, *19*, 3127.

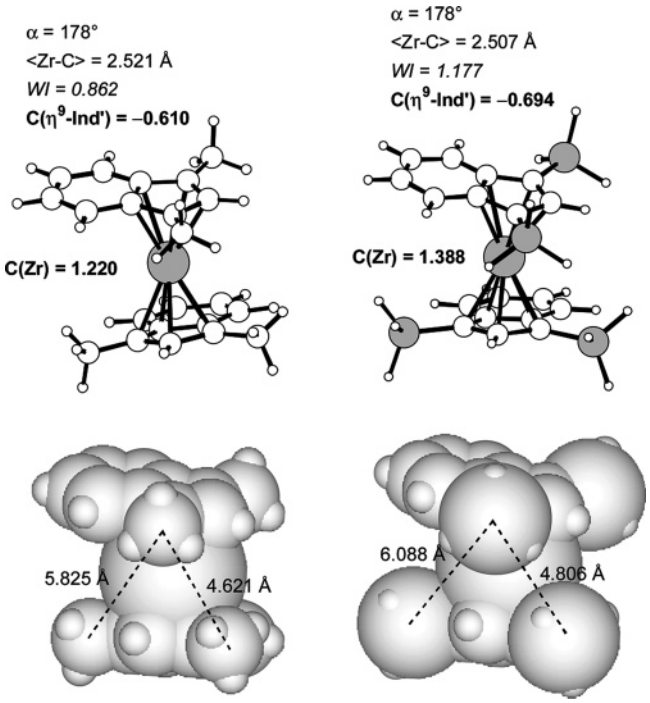

Figure 3. Optimized geometries (B3LYP) for [Zr(η^5-C_9H_5-1,3-CH_3)$_2$] (left) and [Zr(η^5-C_9H_5-1,3-SiH_3)$_2$] (right). The more relevant geometrical and electronic parameters are presented: the NPA charge for the metal and the ligands (C, in bold), the folding angle of the ligand (α, in deg), the mean distance for all the Zr−C bonds (⟨Zr−C⟩, in Å), and the corresponding sum of Wiberg indices (WI, in italics). The Zr and Si atoms are shaded. Space-filling representations are present in the bottom with indication of the C−C (left) and Si−Si (right) distances between the closest indenyl substituents.

case of complex **1** even surpasses the effect of a stronger η^5-Ind′ donor, ending up with a more positive metal in this molecule. In short, for the alkylated Ind′ ligand the η^9 coordination produces stronger metal−ligand bonds, resulting, thus, in more difficult η^9 to η^5 shifts and in slower ligand interchange reactions.

The optimized geometries for spin singlet η^5/η^5 intermediates (**B**) of complexes **1** and **2** are presented in Figure 3 with the more relevant geometrical and electronic parameters.

Both complexes in Figure 3 are typical metallocenes with two η^5-coordinated π ligands. The better donor capability of the methylated ligands, with respect to the silylated indenyls, is reflected in the charge distribution of the two molecules. The complex having indenyl ligands with methyl substituents has less negative ligands and, consequently, a more electron-rich metal center than the silylated species. Nevertheless, the Zr−C bonds are stronger in the silylated molecule, due to significantly shorter distances.[31a] In fact, η^5-coordinated Ind′ ligands with silyl substituents approach the metal at closer distances than methylated indenyls, as a consequence of reduced interligand steric repulsion. Even with two Ind′ ligands closer to each other,[31b] the distance between Ind′ substituents in the two ligands of the molecule is larger in the case of the silylated complex,

(31) (a) This is shown by the mean distances present in Figure 3, as well as by the distances between the metal and the C_5 ring centroids: 2.19 and 2.21 Å for the silylated and the methylated species, respectively. (b) The distance between the two C_5 ring centroids is 4.34 Å for R = R′ = SiH_3 and 4.37 Å for R = R′ = CH_3. (c) Larger Si−C (1. 86 Å) and Si−H (1.49 Å) distances in the silylated ligands, when compared with the corresponding C−C (1.50 Å) and C−H (1.10 Å) in the methylated Ind′, result in a wider distribution of the substituents in the space around the metal for the silylated compounds and allow the establishment of shorter Zr−C(Ind′) bonds.

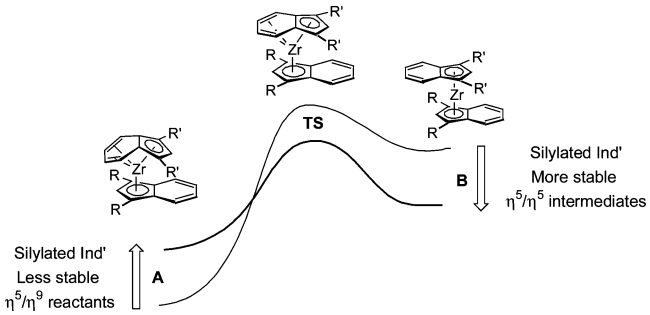

Figure 4. General representation of the influence of the type of substituent on Ind′ in the rate-limiting step of the ligand interchange reaction for [Zr(η^5-Ind′)(η^9-Ind′)] sandwich complexes.

resulting in a less crowded metal coordination sphere, as shown by the space-filling representations in the bottom of Figure 3.[31c] The outcome, in terms of the haptotropic shift reaction, is that, for silylated complexes, the η^5/η^5 intermediates are less destabilized with respect to the η^5/η^9 reactants than in the case of methylated molecules. This, associated with the stronger Zr−(η^9-Ind′) bonds and, thus, the ground-state stabilization of the η^5/η^9 molecules existing in the case of methylated ligands, discussed above, justifies the more facile ligand rearrangement reaction observed for silylated [Zr(η^5-Ind′)(η^9-Ind′)] sandwich complexes (see Figure 4).

The nature of the transition state for the rate-limiting step of the rearrangement reaction (**TS**), concerning its energy and geometry, is directly related with the stability difference between the two species connected, the η^5/η^9 reagent (**A**) and the η^5/η^5 intermediate (**B**), following Hammond's postulate. This is best seen comparing the transition states optimized for complexes **1** and **2**. In both cases **TS** presents one η^5-Ind′, while the shifting ligand has a coordination mode between η^9 and η^5. However, in the case of the silylated complex (**2**) the stability difference between the two minima involved (**A** and **B**) is only 4.5 kcal mol^{-1} and the **TS** is closer to the reactant than in the case of the methylated species (**1**), where that difference is 9.5 kcal mol^{-1}. This is shown by the folding angle of the slipping ligand in **TS**: α = 165° and 162°, for **1** and **2**, respectively. This means that the reactant has to move further in the reaction coordinate to reach the transition state in the case of **1** and, thus, has to overcome a higher energy barrier (12.2 vs 10.4 kcal mol^{-1}).

Another aspect of importance is the performance of the theory model as a function of the nature of the models used in the study. Although any discussion should be taken with caution given the simplicity of the substituents used in this work, a few conclusions may be drawn. The first is that in all cases studied the rate-limiting step corresponds to the η^9 to η^5 shift along the spin singlet PES. This was already observed in the case of the sandwich complex with unsubstituted ligands[24] and is maintained with the substituents here studied. In addition, the activation energies calculated, comprising all cases, are very consistent (within 2.8 kcal mol^{-1}) and compare reasonably well with the experimental activation enthalpies (14.5−20.4 kcal mol^{-1}).[18] Thus, at least in terms of the general conclusions, the theory level seems to perform well, not being too sensitive to the simplicity of the models used. However, significant differences in the relative stability of the η^5/η^5 intermediates (**B**) with respect to the η^5/η^9 reactants (**A**) are observed, as a function of the Ind′ substituents. This causes changes in the shape of the potential energy surfaces near the crossing points that are reflected in the energies of the MECP obtained. This is especially true for **CP** since these crossing points connect the two η^5/η^5 species, the spin singlet **B**, and the spin triplet **C**. A

maximum variation of almost 10 kcal mol^{-1} can be observed in Table 1 for the energies of **CP**. Thus, any conclusion based on the energies of the MECP, especially **CP**, should be taken with caution, given their observed dependence on the indenyl substituent. Although this is not the case for the rearrangement reaction, since **CP** never corresponds to the rate-limiting step of that reaction, that dependence can be of importance in other conclusions such as in the outcome of the alkane reductive elimination reaction from [Zr(η^5-Ind′)(R)(H)] yielding the [Zr(η^5-Ind′)(η^9-Ind′)] sandwich complexes, when performed in the presence of σ donors such as THF. In this reaction a η^5/η^5 species (**B** or **C**) is formed, and the subsequent evolution toward a η^5/η^6 adduct with THF with a spin singlet state versus a spin triplet η^5/η^5 THF adduct depends on the relative energy of **TS** and **CP**. Here the presence of Ind′ substituents may be of crucial importance, and the conclusions based on the results obtained with unsubstituted ligands are, most likely, wrong.[24]

THF Exchange in [Zr(η^5-Ind′)(η^6-Ind′)(THF)] Adducts. The reactivity of [Zr(η^5-Ind′)(η^9-Ind′)] sandwich complexes toward the formation of adducts with σ donors, such as THF, was systematically studied as a function of Ind′ substituents.[22] The results indicate that complexes with silylated Ind′ undergo THF addition preferentially over molecules with alkylated ligands, in good agreement with the influence of the indenyl substituents on the ease of the haptotropic shift, discussed above. The thermodynamics and the kinetics of the equilibrium for THF exchange were also studied by Chirik et al., and two competitive processes could be found, one at work for low THF concentrations and another occurring for higher concentrations. The former corresponds to the formation of the THF adduct from the [Zr(η^5-Ind′)(η^9-Ind′)] sandwich complex, and its mechanism and associated energy profile have been previously reported.[24] The second process corresponds to exchange between free THF and the [Zr(η^5-Ind′)(η^6-Ind′)(THF)] adduct. This reaction was found to be very fast, even on the NMR time scale, and since the experimental data indicate an associative mechanism, a bis(THF) intermediate was postulated, but could not be detected.[22] The calculated energy profile for both processes is represented in Figure 5a.

The THF exchange in the [Zr(η^5-Ind)(η^6-Ind)(THF)] adduct (**F**) can follow a dissociative mechanism, describing the equilibrium between that species and the [Zr(η^5-Ind)(η^9-Ind)] sandwich complex (**E**). This is the process represented on the left side of Figure 5a, and the activation energy calculated (13.6 kcal mol^{-1})[24] agrees with a fluxional behavior in solution at room temperature. A competitive pathway involving an associative mechanism with addition of a second THF molecule (represented in dark gray in Figure 5) was also investigated, and a bis(THF) adduct, **G**, could be optimized, along with the corresponding transition state (**TS$_{FG}$**). The activation energy involved (0.7 kcal mol^{-1}) corroborates a very fast process. The difference between the energy barriers for the two pathways in Figure 5a reflects the geometric changes associated with each mechanism. The dissociative path involves the haptotropic shift of one indenyl ligand from the η^9 coordination mode in **E** ($\alpha = 146°$) to a η^6-Ind in the adduct with a flat ligand ($\alpha = 179°$) bonded by the benzene ring. On the other hand, the associative mechanism involves only minor structural changes, especially in the bond lengths of the ligands already present in **F**.[32]

(32) In the case of the dissociative mechanism, the distortion of the shifting Ind ligand is still present in the transition state **TS$_{EF}$** ($\alpha = 157°$), and the incoming THF ligand is far from the metal center ($d_{Zr-O} = 3.63$ Å) representing an early transition state. For the associative path, the Zr−O bond distance in **F** (2.32 Å) is unchanged in the transition state (**TS$_{FG}$**), and the η^5/η^6 coordination of the Ind ligands is maintained along the reaction.

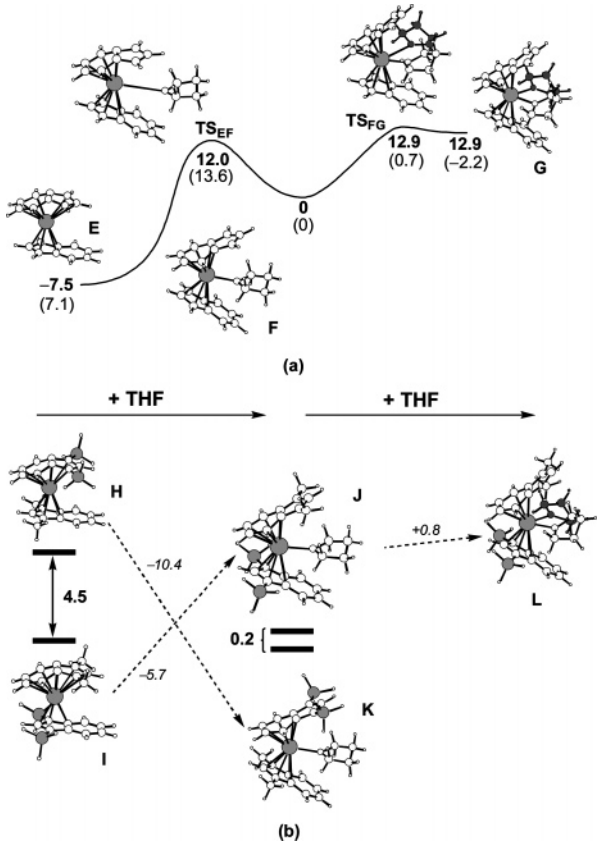

Figure 5. (a) Free energy profile for the mechanism of THF exchange for [Zr(Ind)$_2$] complexes with unsubstituted ligands. The stationary points were optimized (B3LYP), and the obtained structures are presented. Free energies (kcal mol^{-1}) are referred to the mono-THF adduct, **F**. Electronic energies (kcal mol^{-1}) are presented in parentheses. The Zr atom (light gray) and the second entering THF molecule (dark gray) are shaded. (b) Optimized geometries (B3LYP) for the minima involved in the THF addition to a [Zr(Ind′)$_2$] complex having one silylated and one alkylated ligand (R = CH_3, R′ = SiH_3). The stability differences (kcal mol^{-1}) and energy variations (italics) presented correspond to electronic energies. The Zr and Si atoms are shaded (light gray) as well as the second THF molecule (dark gray).

Since the mechanisms studied for the THF exchange correspond to bimolecular reactions, the comparison between the two possible pathways is better performed in terms of free energy in order to account for entropy changes. The values calculated for the activation free energy in the two cases, differing by 0.9 kcal mol^{-1}, are in good agreement with two competitive processes, experimentally observed. In addition, a very shallow minimum associated with the bis(THF) adduct, **G**, isoenergetic with **TS$_{FG}$**, indicates a very reactive intermediate and justifies the failure in the experimental attempts to detect [Zr(η^5-Ind′)(η^6-Ind′)(THF)$_2$] complexes.[22]

Interestingly, slightly longer Zr−O bonds (2.44 Å) are observed in **G**, when compared to the one in the mono-THF adduct, **F** (2.32 Å). This is the result of electronic saturation in the metal center, being in agreement with the differences found in the corresponding distances, comparing the experimental structures of adducts with chelating diethers and mono-THF complexes.[22]

The influence of Ind′ substituents on the addition of THF to [Zr(η^5-Ind′)(η^9-Ind′)] sandwich complexes was studied using a molecule with one silylated and one methylated ligand (R = CH_3 and R′ = SiH_3), and the optimized structures obtained are represented in Figure 5b. In this case only the minima were

calculated, due to computational limitations. The *anti* conformers of the η^5/η^9 molecules (**H** and **I**) were considered, since this is the preferred conformation for the reaction, and the rotation of the Ind′ ligands is known to be a facile process.[18,24] The haptomer with a η^9 coordination of the methylated Ind′ (**I**) is 4.5 kcal mol^{-1} more stable than the species with a η^9-silylated indenyl (**H**). The enhanced donor characteristics of a methylated η^9-Ind′ (in **I**), when compared to a silylated η^9-Ind′ (in **H**), is shown by the NPA charges of those ligands, −0.671 in **I** and −0.784 in **H**, revealing a less negative ligand in the former molecule. This results in a more tightly bond η^9-methylated ligand, with shorter and stronger Zr−C bonds, and, consequently, a more stable haptomer (**I**).[33]

Two practically isoenergetic haptomers were optimized for the THF adducts of the complex with substituted indenyls, **J** and **K**, revealing that the stability difference observed in the parent sandwich complex is not maintained after THF addition. This corroborates the experimental observation that the preference of alkylated indenyls for a η^9 coordination, in the η^5/η^9 molecules, is not translated to the η^5/η^6 THF adducts. The negligible energy difference calculated for **J** and **K** is also indicative that a thermodynamic control for the reaction should exist in the cases where THF addition is fast and reversible in solution, at room temperature, and supports the possibility of observing mixtures of haptomers of adducts with inequivalent indenyl ligands, [Zr(η^5-Ind′)(η^6-Ind″)(THF)] and [Zr(η^5-Ind″)-(η^6-Ind′)(THF)], even when the corresponding sandwich complex exists mainly as one isomer.[22]

The reasons for the comparable stability of **J** and **K** can be found in an analysis of the electronic structure and bonding of the two molecules. Given the differences in η^9-Ind′ coordination discussed above for **H** and **I**, the shift from η^9 to η,[5] that is, the breaking of the three allylic bonds, is more difficult for an alkylated than for a silylated indenyl since the former is a better donor (see the energy variations in Figure 5b). Despite the fact that a electron poorer metal is obtained for **K** (C_{Zr} = 1.394 vs 1.316 in **J**), the presence of a THF ligand plays a decisive role in the stability difference between the two haptomers. The Zr−O bond existing in **K** is shorter (2.309 Å) and stronger (WI = 0.245) than the one observed in the other isomer, **J** (d_{Zr-O} = 2.329 Å and WI = 0.236). Thus, a electron poorer metal in **K** is partially compensated by a stronger Zr−THF bond, and, as a consequence of an increased σ donation, the THF ligand is more positive in **K** (C_{THF} = 0.144) than in **J** (C_{THF} = 0.141). In addition, a synergetic effect occurs and an increased donation from THF corresponds to an increased back-donation from the metal to the η^6-Ind′. This is shown by the NPA charges of the η^6-Ind′ in the two molecules (−1.046 in **K** and −0.839 in **J**), as well as by the strength of the Zr−(η^6-Ind′) bonds, indicated by the sum of Wiberg indices corresponding to the six Zr−C bonds (1.859 for **K** and 1.808 for **J**). In short, a tuning of the Zr−O bond results in an energetic balance between the two isomers, allowing minimal stability differences between species with distinct metal electronic richness. This result is corroborated by the Zr−O bond distances observed in the three X-ray structures published for [Zr(η^5-Ind′)(η^6-Ind′)(THF)] adducts,[22] where a trend may be found correlating shorter Zr−O distances with electronic poorer metal centers, although the differences in bond lengths are quite small (within 0.03 Å).

The bis(THF) adduct was also calculated for the isomer with a methylated η^6-Ind′, and the optimized structure obtained is represented in Figure 5b (**L**). The small energy variation involved in the addition of a second THF molecule from **J** to **L** (+0.8 kcal mol^{-1}) indicates that a THF exchange process involving an associative mechanism should be facile, similarly to what was found with the unsubstituted model (see above). However, in the case of the molecule with substituted ligands, the reaction is slightly endoenergetic, while for the unsubstituted model (from **F** to **G**) it is clearly exoenergetic (ΔE = −2.2 kcal mol^{-1}). This reflects the stereochemical repulsion caused by the Ind′ substituents in a crowded metal center. Comparing the substituted bis(THF) complex, **L**, with its unsubstituted analogue (**G**), the mean Zr−O distance is 0.02 Å longer, the mean Zr−C bond length for the two hinge carbon atoms of the coordinated benzene ring is 0.04 Å longer, and the x−Zr−y angle is 0.5° narrower (x and y represent the centroids of the coordinated rings). In the case of the real molecules, with much larger substituents than the models used in this work, an increased destabilization of the bis(THF) complex with respect to the mono-THF adduct is expected.

Conclusions

Haptotropic shifts of indenyl ligands from η^9 to η^5 coordination are more facile in [Zr(η^5-Ind′)(η^9-Ind′)] complexes with silylated ligands than in equivalent molecules with alkylated Ind′. This results from the combination of two factors. On one hand, alkylated ligands are better electron donors and, thus, make stronger Zr−Ind′ bonds, with a consequent ground-state stabilization of sandwich complexes. On the other, bis(η^5-Ind′) metallocenes are less destabilized in the case of silylated Ind′ ligands due to reduced interligand repulsion. The overall result is that the ligand interchange process between the two inequivalent Ind′ in [Zr(η^5-Ind′)(η^9-Ind′)] is easier for silylated molecules than for their alkylated analogues.

The preference for η^9 coordination of alkylated Ind′ ligands over their silylated counterparts in [Zr(Ind′)$_2$] is not translated to the [Zr(η^5-Ind′)(η^6-Ind′)(THF)] adducts, for molecules with mixed Ind′ ligands. In this case, a tuning of the Zr−O bond compensates the metal electronic needs, leveling the stability differences that would arise from the η^9 to η^6 shift of indenyl ligands with distinct substituents.

Computational Details

All calculations were performed using the Gaussian 98 software package[34] and the B3LYP hybrid functional, without symmetry

(33) The Zr to η^9-Ind′ back-donation involves only the benzene ring of the ligand, and, thus, the distinction in donor capability of the ligand is reflected mainly in the three allylic bonds of the C_5 ring, where the coordination is essentially based on ligand to metal donation. A slightly more folded geometry exists for the methylated Ind′ in **I** (α = 146°), when compared with the η^9 ligand in **G** (α = 147°). Since the Zr−C bonds associated with the benzene ring of η^9-Ind′ are similar in the two molecules (within 0.01 Å), the difference results from the Zr−C bonds to the three allylic carbons of the C_5 ring of each ligand, being shorter in the case of the methylated ligand in **I** (2.666, 2.671, and 2.866 Å) than for the silylated indenyl in **H** (2.699, 2.700, and 2.897 Å). This indicates a stronger donation from η^9-Ind′ to Zr for the methylated ligand and defines the stability difference found between **H** and **I**.

(34) Frisch, M. J.; Trucks, G. W.; Schlegel, H. B.; Scuseria, G. E.; Robb, M. A.; Cheeseman, J. R.; Zakrzewski, V. G.; Montgomery, J. A., Jr.; Stratmann, R. E.; Burant, J. C.; Dapprich, S.; Millam, J. M.; Daniels, A. D.; Kudin, K. N.; Strain, M. C.; Farkas, O.; Tomasi, J.; Barone, V.; Cossi, M.; Cammi, R.; Mennucci, B.; Pomelli, C.; Adamo, C.; Clifford, S.; Ochterski, J.; Petersson, G. A.; Ayala, P. Y.; Cui, Q.; Morokuma, K.; Malick, D. K.; Rabuck, A. D.; Raghavachari, K.; Foresman, J. B.; Cioslowski, J.; Ortiz, J. V.; Stefanov, B. B.; Liu, G.; Liashenko, A.; Piskorz, P.; Komaromi, I.; Gomperts, R.; Martin, R. L.; Fox, D. J.; Keith, T.; Al-Laham, M. A.; Peng, C. Y.; Nanayakkara, A.; Gonzalez, C.; Challacombe, M.; Gill, P. M. W.; Johnson, B. G.; Chen, W.; Wong, M. W.; Andres, J. L.; Head-Gordon, M.; Replogle, E. S.; Pople, J. A. *Gaussian 98*, revision A.7; Gaussian, Inc.: Pittsburgh, PA, 1998.

constraints. That functional includes a mixture of Hartree−Fock[35] exchange with DFT[23] exchange−correlation, given by Becke's three-parameter functional[36] with the Lee, Yang, and Parr correlation functional, which includes both local and nonlocal terms.[37,38] The LanL2DZ basis set[39] augmented with a f-polarization function[40] was used for Zr, and a standard 6-31G(d,p)[41] for the remaining elements. Transition-state optimizations were performed with the synchronous transit-guided quasi-Newton method (STQN) developed by Schlegel et al.[42] Frequency calculations were performed to confirm the nature of the stationary points, yielding one imaginary frequency for the transition states and none for the minima. Each transition state was further confirmed by following its vibrational mode downhill on both sides and obtaining the minima presented on the energy profile. The minimum energy crossing points (MECP) between the spin singlet ($S = 0$) and the spin triplet ($S = 1$) potential energy surfaces (PES) were determined using a code developed by Harvey et al.[43] This code consists of a set of shell scripts and Fortran programs that uses the Gaussian results of energies and gradients of both spin states to produce an effective gradient pointing toward the MECP. Spin contamination was carefully monitored for all the unrestricted calculations performed for the triplet species (**C**) and the open-shell singlets, i.e., all the η^5/η^5 species with $S = 0$ (**B**), and the transition states for the η^9 to η^5 shifts (**TS**), along the $S = 0$ PES. The values of $\langle S^2 \rangle$ indicate minor spin contamination and are presented in the Supporting Information. The energy values discussed along the text are not zero-point-corrected since, on one hand, the maximum deviation between the zero-point-corrected and the uncorrected energies is 0.7 kcal mol^{-1}, all the stationary points considered, and, on the other, MECP are not stationary points and a standard frequency analysis is not applicable.[43] The free energies were obtained at 298.15 K and 1 atm by conversion of the zero-point-corrected electronic energies with the thermal energy corrections based on the calculated structural and vibrational frequency data. A natural population analysis (NPA)[27] and the resulting Wiberg indices[28] were used for a detailed study of the electronic structure and bonding of the optimized species.

The theoretical method used in this work was thoroughly tested in the previous study involving [Zr(η^5-Ind)(η^9-Ind)] complexes with unsubstituted indenyl ligands.[24] Basis set convergence, in size, was confirmed by comparing optimized geometries and energies obtained with the basis set here employed (VDZP) with the corresponding results yielded by a VTZP basis set. In addition, the influence of the functional used, and, in particular, the amount of exact exchange included, was also tested. This factor is known to be of relevance in the evaluation of the relative stability of different spin states for organometallic complexes of transition metals.[44,45]

Acknowledgment. The author is thankful to Dr. Paul J. Chirik for sharing data prior to publication and for helpful suggestions.

Supporting Information Available: Tables of atomic coordinates for all the optimized species. This material is available free of charge via the Internet at http://pubs.acs.org.

OM051085L

(35) Hehre, W. J.; Radom, L.; Schleyer, P. v. R.; Pople, J. A. *Ab Initio Molecular Orbital Theory*; John Wiley & Sons: New York, 1986.
(36) Becke, A. D. *J. Chem. Phys.* **1993**, *98*, 5648.
(37) Miehlich, B.; Savin, A.; Stoll, H.; Preuss, H. *Chem. Phys. Lett.* **1989**, *157*, 200.
(38) Lee, C.; Yang, W.; Parr, G. *Phys. Rev. B* **1988**, *37*, 785.
(39) (a) Dunning, T. H., Jr.; Hay, P. J. *Modern Theoretical Chemistry*; Schaefer, H. F., III, Ed.; Plenum: New York, 1976; Vol. 3, p 1. (b) Hay P. J.; Wadt, W. R. *J. Chem. Phys.* **1985**, *82*, 270. (c) Wadt W. R.; Hay, P. J. *J. Chem. Phys.* **1985**, *82*, 284. (d) Hay P. J.; Wadt, W. R. *J. Chem. Phys.* **1985**, *82*, 2299.
(40) Ehlers, A. W.; Böhme, M.; Dapprich, S.; Gobbi, A.; Höllwarth, A.; Jonas, V.; Köhler, K. F.; Stegmann, R.; Veldkamp A.; Frenking, G. *Chem. Phys. Lett.* **1993**, *208*, 111.
(41) (a) Ditchfield, R.; Hehre W. J.; Pople, J. A. *J. Chem. Phys.* **1971**, *54*, 724. (b) Hehre, W. J.; Ditchfield R.; Pople, J. A. *J. Chem. Phys.* **1972**, *56*, 2257. (c) Hariharan, P. C.; Pople, J. A. *Mol. Phys.* **1974**, *27*, 209. (d) Gordon, M. S. *Chem. Phys. Lett.* **1980**, *76*, 163. (e) Hariharan, P. C.; Pople, J. A. *Theor. Chim. Acta* **1973**, *28*, 213.
(42) (a) Peng, C.; Ayala, P. Y.; Schlegel, H. B.; Frisch, M. J. *J. Comput. Chem.* **1996**, *17*, 49. (b) Peng, C.; Schlegel, H. B. *Isr. J. Chem.* **1994**, *33*, 449.
(43) Harvey, J. N.; Aschi, M.; Schwarz, H.; Koch, W. *Theor. Chem. Acc.* **1998**, *99*, 95.
(44) Harvey, J. N. *Struct. Bonding* **2004**, *112*, 151.
(45) Harvey, J. N.; Aschi, M. *Faraday Discuss.* **2003**, *124*, 129.